Lateral Mean Exit Time of a Spherical Particle Trapped in an Optical Tweezer

Ranaweera, Aruna; Åström, Karl Johan; Bamieh, Bassam

Published in:
Decision and Control, 2004. CDC. 43rd IEEE Conference on

2004

43rd IEEE Conference on Decision and Control
December 14-17, 2004
Atlantis, Paradise Island, Bahamas

Lateral Mean Exit Time of a Spherical Particle Trapped in an Optical Tweezer

Aruna Ranaweera
ranawera@engineering.ucsb.edu

Karl J. Åström
astrom@engineering.ucsb.edu

Bassam Bamieh
bamieh@engineering.ucsb.edu

Department of Mechanical and Environmental Engineering, University of California, Santa Barbara, CA 93106-5070

***Abstract*— We apply the Fokker-Planck equation to analyze the stochastic behavior of a 1-micron diameter polystyrene bead trapped in water using an optical tweezer. Due to thermal noise, given enough time, a trapped particle will escape confinement from the trap. However, at biological temperatures, for laser powers of greater than approximately 5 milliwatts at the focus, the mean first exit time in the lateral plane is extremely large, and unbounded for most practical purposes. We show that the mean exit time increases exponentially with laser power. Furthermore, for a trapped 9.6-micron diameter polystyrene bead, we show that experimental mean passage times within the linear trapping region are in close agreement with theoretical calculations.**

I. Introduction

The optical tweezer is a device that uses a focused laser beam to trap and manipulate individual dielectric particles in an aqueous medium. The laser beam is sent through a high numerical aperture (highly converging) microscope objective that is used for both trapping and viewing particles of interest. Several milliwatts of laser power at the focus can generate trapping forces on the order of piconewtons, which is well suited for biomolecular studies. Although biological molecules are too small to be trapped at room temperature, a molecule can be grasped once a trappable 'handle', such as a polystyrene bead, is (biochemically) attached to that molecule [1].

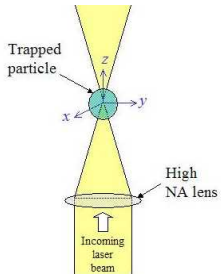

Fig. 1. Basic optical tweezer. A single laser beam is focused to a diffraction-limited spot using a high numerical aperture microscope objective. Dielectric particles are trapped near the laser focus.

Although optical tweezers have been used to trap dielectric particles with diameters in the range of tens of nanometers to tens of microns, strongest trapping is expected for particles that are roughly the same size as the laser wavelength [1], [2]. Since the most commonly used laser wavelength in biological experiments is 1064 nm, this paper will investigate the trapping behavior of polystyrene beads of diameter 1 μm. For small enough displacements from the center of the trap (up to approximately 200 nm) [3], the optical tweezer can be modeled as a Hookeian spring, characterized by a fixed trap-stiffness [4]. For larger displacements from the center of the trap (up to the maximum trapping radius R of approximately 675 nm), the optical tweezer behaves like a nonlinear restoring spring [3]. led as a Hookeian spring, characterized by a fixed trap-stiffness [4]. For larger displacements from the center of the trap (up to the maximum trapping radius R of approximately 675 nm), the optical tweezer behaves like a nonlinear restoring spring [3].

The performance of an optical trap can be characterized in several ways. Within the linear trapping region, parameters such as trap stiffness and characteristic frequency are commonly used, whereas within the nonlinear (entire) trapping region, the maximum trapping force is often used [4], [5], [6]. In this paper, we will investigate first exit times, which tell us how long a particle will remain within the optical trap. For a given optical tweezer configuration, the first exit time is an extremely useful measure of trapping capability because it quantifies the time horizon during which experiments can be conducted before trapped particles are lost; although high-quality microscope objectives are capable of handling laser power levels of up to approximately 500 mW at the focus, typical biological optical tweezer experiments use much lower power levels; it is especially important to use lower power levels when studying biological samples to avoid damaging them with heat, which is known as 'opticution' [7]. Furthermore, in applications in which the power from a single laser beam is shared by many traps, the power available for each trap can be very small; in this situation, it is useful to understand and quantify the lowest power levels that are capable of providing sufficiently strong traps.

In the remaining sections of this paper, we describe the equation of motion of a spherical particle trapped in an optical tweezer. We then apply the Fokker-Planck

0-7803-8682-5/04/$20.00 ©2004 IEEE

equation to investigate the probability distribution and lateral mean first exit time of a trapped 1-μm diameter polystyrene bead. We show that, for a 9.6-μm diameter bead trapped within the linear trapping force region, mean passage times according to experimental data are in close agreement with theoretical calculations.

II. Modeling

A. Equation of Motion

The equation of motion along the lateral x-axis for a trapped bead of mass m and lateral position x is given by

$$m\ddot{x} = F_T(x_r) + F_D(\dot{x}) + F_L(t), \tag{1}$$

where $F_T(\cdot)$ is the optical trapping force, $F_D(\cdot)$ is the viscous drag, and $F_L(t)$ is a Langevin (random thermal) disturbance force. The relative position x_r is defined as

$$x_r := x - x_T, \tag{2}$$

where x_T is the trap (laser focus) position. For relative displacements within the trapping radius R, the trap can be modeled as a cubic restoring spring:

$$F_T = \begin{cases} \alpha_3 x_r^3 - \alpha_1 x_r & \text{for } |x_r| < R = \sqrt{\frac{\alpha_1}{\alpha_3}} \\ 0 & \text{otherwise.} \end{cases} \tag{3}$$

Figure 2 shows a typical cubic trapping force model in which $\alpha_3 = 22$ pN/μm^3, $\alpha_1 = 10$ pN/μm, and $R = 0.674$ μm. The nonlinear spring constants α_1 and α_3 were obtained by fitting a cubic polynomial to experimental results published by Simmons et al. [3].

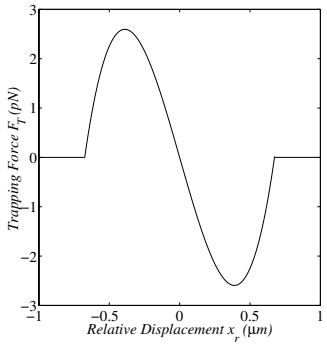

Fig. 2. Cubic trapping force model for a 1-μm diameter polystyrene bead, based on experimental results from [3], in which laser power is approximately 100 mW at the focus ($\rho = 1$).

It should be mentioned that an optical tweezer traps particles in not only one, but three dimensions (Figure 1). For a well-aligned trap, the trapping profile is cylindrically symmetric about the axial z direction in which laser light propagates. As a result, ignoring polarization effects, the optical trapping force along the lateral y axis is identical to that along the lateral x axis. However, the trapping force in the x direction is not invariant with respect to motion along the y axis [6]. Therefore, when considering motion in a lateral plane, it is convenient to use polar coordinates instead of Cartesian coordinates. In the remainder of this paper, we will interpret the spatial coordinate x as representing radial position in the lateral plane from the center of the trap.

The trapping force of an optical tweezer is proportional to the laser power [8]. In the remainder of this paper, we will denote the laser power by the factor $\rho > 0$, which is defined relative to the power level used in [3]. In particular, $\rho = 1$ corresponds to approximately 100 mW at the focus. The trapping force also increases with numerical aperture, so the force model (3), and therefore, the material in this paper, are quantitatively accurate for a 1.25 NA (numerical aperture) microscope objective, which was used in [3]. However, as shown in [9], the trapping force for a spherical particle always has a profile that qualitatively matches (3). Therefore, our results can be extended qualitatively to higher numerical apertures (for example, NA = 1.30 or 1.40), if necessary.

The drag force can be expressed as

$$F_D = -\beta\dot{x}, \tag{4}$$

where $\beta > 0$ is the viscous damping factor given by Stoke's equation, $\beta = 6\pi\eta r_b$, in which r_b is the bead radius and η is the fluid viscosity. For a 1-μm bead trapped in water at room temperature, $\beta \approx 0.01$ pNs/μm. The power fraction ρ, (1), (3), and (4) can be combined to obtain the equation of motion for a trapped particle:

$$m\ddot{x} = \rho\psi(x_r)(\alpha_3 x_r^3 - \alpha_1 x_r) - \beta\dot{x} + F_L(t), \tag{5}$$

in which

$$\psi(x_r) := \begin{cases} 1 & \text{for } |x_r| < R \\ 0 & \text{otherwise.} \end{cases} \tag{6}$$

Along one axis, the Langevin force has an average value of zero and a constant, one-sided power spectrum (i.e., ideal white noise force) given by $S_L^+(f) = 4\beta k_B T$, where k_B is Boltzmann's constant and T is absolute temperature [5]. Correspondingly, denoting the Dirac delta function by $\delta(t)$, the covariance $r_L(t)$ of the radial Langevin force is given by

$$r_L(t) = R_L\delta(t) = 2\beta k_B T\delta(t), \tag{7}$$

since $R_L = \frac{1}{2}S_L$, in magnitude [10]. At biological temperatures, $k_B T = 4 \times 10^{-3}$ pNμm [5]. Hence, for a 1-μm polystyrene bead trapped at room temperature, $R_L \approx 8 \times 10^{-5}$ μm^2.

In practice, the mass of the trapped particle is small enough that it can be ignored. For example, for a 1-μm diameter polystyrene bead, $m \approx 5.5 \times 10^{-10}$ mg, and the characteristic frequency (bandwidth) ω_c of the trap (with the force profile shown in Figure 2) is given by $\omega_c \leq \frac{\alpha_1}{\beta} = 1$ krad/s. Therefore, (5) can be simplified to

obtain the noninertial equation of motion for a trapped particle at low Reynolds' number:

$$0 = \rho\psi(x_r)(\alpha_3 x_r^3 - \alpha_1 x_r) - \beta\dot{x} + F_L(t). \quad (8)$$

B. State Model

By defining trap position as the control input, $u := x_T$, we can express (8) by the state model:

$$\begin{aligned} \dot{x} &= \rho\frac{\psi(x-u)}{\beta}\big[\alpha_3(x-u)^3 - \alpha_1(x-u)\big] + \frac{F_L}{\beta} \\ y &= x. \end{aligned} \quad (9)$$

Therefore, the open loop differential equation is given by

$$\dot{x} = \rho\frac{\psi(x)}{\beta}\big[\alpha_3 x^3 - \alpha_1 x\big] + \frac{F_L}{\beta}. \quad (10)$$

Because it does not account for angular position θ, the state form (9) is not a complete state space description. For the purposes of this paper, however, we are not concerned with angular position. Comparing (10) with the standard state form from [10],

$$\dot{x} = f(x,t) + \sigma(x,t)e(t), \quad (11)$$

in which $e(t)$ is white noise with covariance $r_e(\tau) = \delta(\tau)$, we see that $f(x,t) = f(x)$ and $\sigma(x,t) = \sigma$ are given by

$$f(x) = \rho\frac{\psi(x)}{\beta}\big[\alpha_3 x^3 - \alpha_1 x\big] \quad (12)$$

$$\sigma = \sqrt{\frac{2k_BT}{\beta}}. \quad (13)$$

For a 1-μm bead trapped in water at room temperature, $\sigma^2 = 0.8\ \mu\mathrm{m}^2$.

C. Stochastic Differential Equation

We can express (9) as a stochastic differential equation:

$$\begin{aligned} dx &= \rho\frac{\psi(x-u)}{\beta}\big[\alpha_3(x-u)^3 - \alpha_1(x-u)\big]dt \\ &\quad + \frac{F_L}{\beta}dt, \end{aligned} \quad (14)$$

which, in the open loop case, simplifies as:

$$dx = \rho\frac{\psi(x)}{\beta}\big[\alpha_3 x^3 - \alpha_1 x\big]dt + \frac{F_L}{\beta}dt. \quad (15)$$

Comparing with the standard state form,

$$dx = f(x,t)dt + \sigma(x,t)dw, \quad (16)$$

in which w is a Wiener process with incremental covariance dt, we see that $f(x)$ and σ are given by (12) and (13).

III. Probability Distribution

Defining $p = p(x,t;x_0,t_0)$ as the probability of being in state x at time t given that the particle was (initially) in state x_0 at time t_0, the conditional distribution p satisfies the Fokker-Planck equation (also known as the Kolmogorov forward equation) given by

$$\frac{\partial p}{\partial t} = -\frac{\partial}{\partial x}(pf) + \frac{1}{2}\frac{\partial^2}{\partial x^2}(\sigma^2 p), \quad (17)$$

where f and σ are defined according to the stochastic differential equation (16) [10]. The initial condition is specified as $p(x,t_0;x_0,t_0) = \delta(x-x_0)$.

A. Transient Distribution

The time-dependent Fokker-Planck equation (17) can be solved numerically, but we have not included the solution in this paper. (Solution procedures can be found in most texts on partial differential equations.)

B. Steady State Distribution

By analyzing the probability distribution in steady-state, we can classify the nature of boundaries for a trapped particle. Substituting $\frac{\partial p}{\partial t} = 0$ into (17), we obtain:

$$\frac{\partial}{\partial x}(pf) = \frac{1}{2}\frac{\partial^2}{\partial x^2}(\sigma^2 p). \quad (18)$$

This can be integrated twice to obtain

$$\ln\left(\frac{p(x)}{p(0)}\right) = \frac{2}{\sigma^2}\int_0^x f(x)dx, \quad (19)$$

assuming $f(0) = 0$ and $\left[\frac{dp}{dx}\right]_{x=0} = 0$. The first assumption is satisfied according to (3), and we will subsequently see that the second assumption also holds. Denoting the integral in (19) as $I(x)$, we can use the expression for $f(x)$ from (12) to show that

$$I(x) = \begin{cases} \rho\frac{x^2}{4\beta}(\alpha_3 x^2 - 2\alpha_1) & \text{for } |x| < R = \sqrt{\frac{\alpha_1}{\alpha_3}} \\ -\rho\frac{\alpha_1^2}{4\beta\alpha_3} & \text{for } |x| \geq R, \end{cases} \quad (20)$$

which is shown graphically in the top plot of Figure 3 for $\rho = 1$ (100 mW) and $\rho = 0.1$ (10 mW). From (19), we see that

$$p(x) = p(0)e^{\frac{2}{\sigma^2}I(x)}, \quad (21)$$

which, combined with (20) and (13) gives

$$p(x) = \begin{cases} p(0)e^{\rho\frac{x^2}{4k_BT}(\alpha_3 x^2 - 2\alpha_1)} & \text{for } |x| < R \\ p(0)e^{-\rho\frac{\alpha_1^2}{4k_BT\alpha_3}} & \text{for } |x| \geq R, \end{cases} \quad (22)$$

which is shown graphically in the bottom plot of Figure 3.

Because the integral $I(x)$ is not negatively unbounded outside of the trapping radius R, the probability density $p(x)$ has a nonzero value for all positions outside of the trapping radius. As a result, if we attempt to normalize $p(x)$ by imposing the condition, $\int_{-\infty}^{\infty} p(x)dx = 1$, we

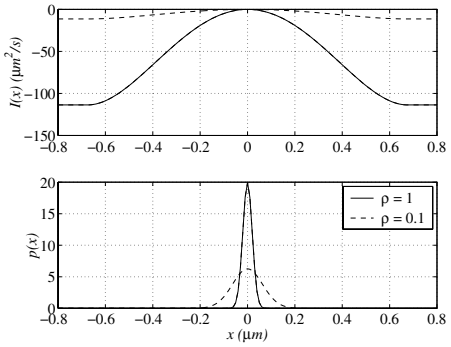

Fig. 3. Normalized steady state probability distribution calculations for $\rho = 1$ and $\rho = 0.1$, assuming finite absorbing boundaries at $x = \pm 50$ μm. In the bottom plot, the nonzero tails of the probability distributions are too small to be seen.

find that $p(x)$ is zero for all x. In other words, in the absence of finite absorbing boundaries, the particle has a finite probability of being anywhere in the radial x-direction (i.e., in the lateral plane), which implies that, given enough time, a trapped particle will escape confinement by the trap and move in a Brownian fashion. In terms of classification of boundary conditions, this implies that a trapped particle has accessible boundaries at all locations in the lateral plane [11].

In practice, the fluid cell which contains trapped particles has lateral dimension of approximately 20 mm and the field of view is typically about 100 μm. Therefore, we can impose absorbing boundaries at $x = \pm 50$ μm, which has been done for the distributions shown in Figure 3.

IV. First Exit Time

In Section III-B, we showed that, in theory, given enough time, a trapped particle will travel beyond the trapping radius R and escape confinement of the trap [11]. Therefore, in the presence of accessible boundaries, we can define the first exit time T_1 as the random variable

$$\begin{aligned} T_1 &= T_1(x_0, -R, R) \\ &:= \sup\{t | X(\tau) \in (-R, R),\ 0 \le \tau \le t\}, \end{aligned} \tag{23}$$

where $X(\tau)$ is the random variable corresponding to particle position x with initial condition $X(0) = x_0$ [11]. In theory, it is possible for a particle to escape from the trap and wander back into it as a result of Brownian motion. Therefore, the 'exit times' described in this paper are not synonymous with 'escape times'; according to our model, a particle never truly escapes from the trap unless it hits a finite absorbing boundary.

A. First Exit Time Distribution

If we define $g = g(t; x_0, -R, R)$ as the probability density function of the first exit time $T_1(x_0, -R, R)$, we can use results from [11] to show that the Laplace transform $G = G(s; x_0, -R, R)$ is given by the expression

$$G(s; x_0, -R, R) = \frac{\epsilon_2(x_0)[\epsilon_1(R) - \epsilon_2(-R)] - \epsilon_1(x_0)[\epsilon_2(R) - \epsilon_2(-R)]}{\epsilon_1(R)\epsilon_2(-R) - \epsilon_1(-R)\epsilon_2(R)}, \tag{24}$$

where $\epsilon_1(x)$ and $\epsilon_2(x)$ are any two linearly independent solutions of the ordinary differential equation

$$\frac{k_B T}{\beta}\frac{d^2\epsilon}{dx^2} + \rho\frac{(\alpha_3 x^3 - \alpha_1 x)}{\beta}\frac{d\epsilon}{dx} - s\epsilon = 0. \tag{25}$$

Obtaining the above density function g of the first exit time requires tedious calculations that are unnecessary for the purposes of this paper. To simplify our analysis, we will investigate the mean first exit time, which can be obtained using much simpler calculations.

B. Mean Exit Time

For our system, the mean first exit time $m_1 := E\{T_1\}$ in the radial x direction is given by the linear second order ordinary differential equation

$$\frac{1}{2}\sigma^2\frac{d^2 m_1}{dx_0^2} + f(x_0)\frac{dm_1}{dx_0} = -1, \tag{26}$$

with two-point boundary conditions, $m_1(-R) = m_1(R) = 0$ [12]. Substituting f and σ from (12) and (13), we obtain:

$$\frac{k_B T}{\beta}\frac{d^2 m_1}{dx_0^2} + \rho\frac{(\alpha_3 x_0^3 - \alpha_1 x_0)}{\beta}\frac{dm_1}{dx_0} + 1 = 0, \tag{27}$$

which can be solved numerically. The mean exit time for $\rho = 1$ (100 mW) is bounded, but extremely large, with a maximum in the vicinity of over 10^{100} trillion years for $x_0 = 0$. This length of time is unbounded for all practical purposes! As shown in Figure 4, reducing the power to $\rho = 0.01$ (1 mW) drastically reduces the mean exit time such that its maximum is approximately 2.51 s at $x_0 = 0$. For comparison, the mean exit time for $\rho = 0$ is 0.57 s, which corresponds to free diffusion of an untrapped particle due to Brownian motion.

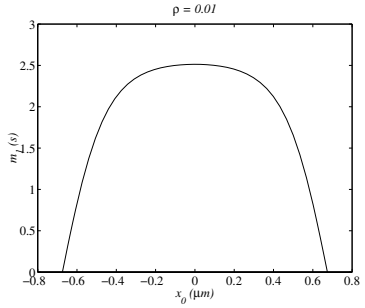

Fig. 4. Mean exit time for $\rho = 0.01$ (1 mW). Maximum is $m_1(0) = 2.51$ s.

Figure 5 shows the maximum mean exit time $m_1(0)$ as a function of the laser power factor ρ for $\rho \le 0.1$

(10 mW). The solid line pertains to a 1-μm diameter polystyrene bead in water at biological temperature ($\sigma^2 = 0.8$ μm^2; $\beta = 0.01$ pNs/μm). For comparison, three other combinations of σ^2 and β have also been plotted. The maximum mean exit time (solid line) for $\rho = 0.05$ (5 mW) is 3.63×10^4 s, or about 10 hours, which is more than sufficient for present-day optical tweezer experiments. (Due to factors such as drift and cross-contamination, typical biological experiments are conducted for not more than a few minutes at a stretch [5], [13]).

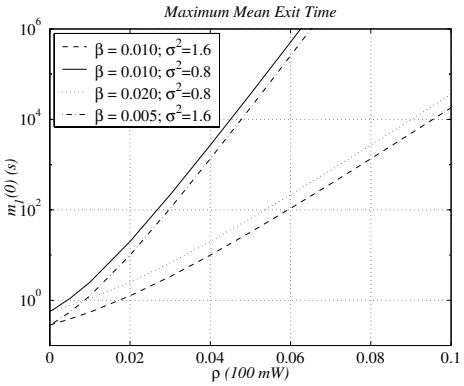

Fig. 5. Maximum mean exit time as a function of laser power factor. The mean exit time increases exponentially with laser power.

According to Figure 5, the maximum mean exit time for $\rho = 0$ appears to be directly proportional to σ^2. That is, with reference to (13),

$$[m_1(0)]_{\rho=0} \propto \sigma^2 \propto \frac{k_B T}{\beta}. \tag{28}$$

Furthermore, for a given value of ρ, the rate of change of the logarithm of the maximum mean exit time (with respect to ρ) appears to be inversely proportional to $\sigma^2\beta$. That is, with reference to (13),

$$\left[\frac{d \log m_1(0)}{d\rho}\right]_{\rho \text{ const.}} \propto \frac{1}{\sigma^2 \beta} \propto \frac{1}{k_B T}. \tag{29}$$

C. Experimental Results

Verifying the theoretical mean exit time results from Section IV-B is difficult for a number of reasons:

1) Typical position detection systems, such as photodetector circuits, are often ineffective beyond the linear trapping region. As a result, real-time position detection at the outskirts of the trapping radius usually requires an imaging system with very high spatial and temporal resolution. Such a system is not available in our laboratory.
2) Once a particle escapes the trap, it will often drift away. To obtain enough measurements of the exit time to make statistically meaningful statements, we would require a system that automatically captures particles and measures their exit times. The alternative would be to manually trap and measure mean exit times, but that is an inaccurate and labor intensive process.
3) The lateral mean exit time calculations do not account for the fact that the particle might escape in the axial direction. A thorough experimental verification of exit times would require an accurate model of the axial trapping force, which is not currently available.

However, we can compute the mean passage time for particles *within the linear region* quite easily by detecting zero crossings and subsequent excursions outside of the radius r of interest. The mean passage time is analogous to the mean exit time, but with R in (23) replaced by $r < R$ [11]. Figure 6 shows how the maximum mean exit time can be calculated for a trapped 9.6-μm bead.

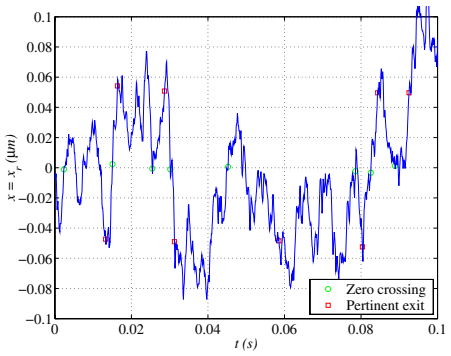

Fig. 6. Calculation of maximum mean exit time from $r = \pm 0.05$ μm for a 9.6-μm polystyrene bead. Green circles depict pertinent zero crossings; Red squares depict pertinent excursions outside of $x_r = \pm 0.05$ μm. Experimental data was sampled at 10 kHz for a total of 30 seconds.

Figure 7 shows the calculated mean passage times for a 9.6-μm diameter bead in a Phosphate-Buffered Saline (PBS) solution, which is used to prevent beads from clumping together. For comparison, theoretical values for $\alpha_1 = 1.81$ pN/μm and $\beta = 0.015$ pNs/μm are also shown. (We assume $\alpha_3 = 0$ within the linear trapping region.) These stiffness and drag values were obtained from a standard power spectrum calibration [6]. Clearly, the theoretical and experimental values are in close agreement. The slight discrepancies for low and high values of r are most likely due to unmodeled nonlinearities in the position detector response; furthermore, experimental mean passage times for low r are artificially inflated due to quantization errors. Although the experimental results in this section pertain to a bead that is much larger than the 1-μm bead studied in the previous sections, the results apply to beads of any size, as long as they remain within the linear region. If we considered the entire nonlinear trapping region, the cubic model (3) would have to be re-scaled; it is unclear how the nonlinear force model should be modified to

accurately account for larger beads.

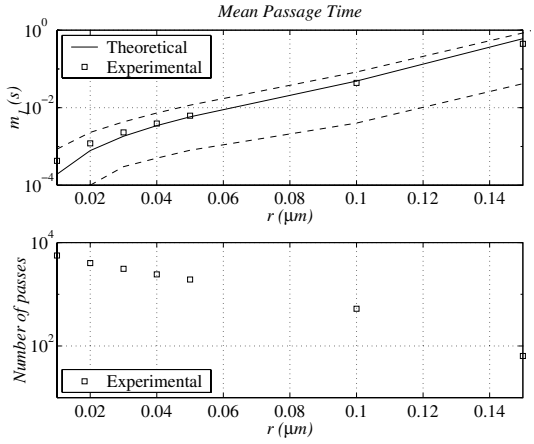

Fig. 7. Maximum mean exit time within the linear region for a 9.6-μm bead. Top plot shows measured mean exit time, including measured standard deviation bounds (dashed lines); bottom plot shows number of pertinent crossings outside of the radius of interest. Theoretical values assume $\alpha = 1.81$ pN/μm and $\beta = 0.015$ pNs/μm; experimental data was sampled at 10 kHz for a total of 30 seconds.

V. Conclusion

In this paper, we applied the Fokker-Planck equation to analyze the stochastic behavior of a spherical particle trapped in an optical tweezer. In theory, given enough time, a trapped particle will escape confinement from the trap. We calculated values for a 1-μm diameter polystyrene bead trapped in water at biological temperature; in particular, for laser powers of greater than approximately 5 mW at the focus, the mean first escape time is extremely large, and unbounded for most practical purposes. With no laser power (i.e., in the absence of an optical trap), the particle moves in a Brownian manner, which has a maximum mean escape time in the radial x direction of just under 0.6 s. We show that the maximum mean exit time increases exponentially with laser power. For a trapped 9.6-μm diameter polystyrene bead, we show that experimental mean passage times within the linear trapping region are in close agreement with theoretical calculations.

As mentioned in Section II-A, the axial trapping force directed toward the microscope objective (in the z direction), will be weaker than the lateral trapping force. Consequently, a trapped particle is more likely to escape in the axial direction away from the microscope objective (in the direction of laser light propagation) than in any other direction. Therefore, if we consider all three spatial dimensions, the actual mean escape times will be less than that for just the lateral plane considered in this paper. In the absence of an experimentally verified trapping force model for the axial z direction, we have not attempted to calculate 3-dimensional exit times in this paper. Instead, we have assumed that trapped particles have been stabilized in the axial z direction. In practice, axial stabilization (within measurement error) can be achieved using low-gain feedback with appropriate sensors and actuators [3], [4].

By casting our system as a stochastic differential equation and using a lateral nonlinear trapping force model of an optical trap, we have developed a framework for studying the stochastic behavior of trapped particles in the lateral plane. This has enabled us to study the mean first exit time, which is an extremely useful measure of the trapping capability of an optical tweezer; it enables system designers to understand and quantify the limitations of using low power levels. Although our (nonlinear) analysis applies specifically to (commonly used) 1-μm diameter polystyrene beads trapped in water using a 1.25 NA microscope objective, the methods used in this paper are applicable to a wide variety of optical tweezer systems, once appropriate adjustments have been made to account for different trapping force profiles (F_T), particle sizes (r_b), fluid properties (β), and temperature (T). We believe that the results of this paper will be useful for designers of optical tweezer systems and experiments.

References

[1] S. Chu, "Laser manipulation of atoms and particles," *Science*, vol. 253, pp. 861–866, 1991.

[2] A. D. Mehta, J. T. Finer, and J. A. Spudich, "Reflections of a lucid dreamer: optical trap design considerations," in *Methods in Cell Biology* (M. P. Sheetz, ed.), vol. 55 (*Laser Tweezers in Cell Biology*), ch. 4, pp. 47–69, Academic Press, 1998.

[3] R. M. Simmons, J. T. Finer, S. Chu, and J. Spudich, "Quantitative measurements of force and displacement using an optical trap," *Biophys. J.*, vol. 70, pp. 1813–1822, 1996.

[4] K. Visscher, S. P. Gross, and S. M. Block, "Construction of multiple-beam optical traps with nanometer-resolution position sensing," *IEEE J. Select. Topics Quantum Electronics*, vol. 2, no. 4, pp. 1066–1076, 1996.

[5] F. Gittes and C. H. Schmidt, "Signals and noise in micromechanical measurements," in *Methods in Cell Biology* (M. P. Sheetz, ed.), vol. 55 (*Laser Tweezers in Cell Biology*), ch. 8, pp. 129–156, Academic Press, 1998.

[6] A. Ranaweera, *Investigations with Optical Tweezers: Construction, Identification, and Control*. PhD thesis, Department of Mechanical and Environmental Engineering, University of California, Santa Barbara, September 2004.

[7] K. Svoboda and S. M. Block, "Biological applications of optical forces," *Annu. Rev. Biophys. Biomol. Struct.*, vol. 23, pp. 247–285, 1994.

[8] S. P. Smith, S. R. Bhalotra, A. L. Brody, B. L. Brown, E. K. Boyda, and M. Prentis, "Inexpensive optical tweezers for undergraduate laboratories," *Am. J. Physics*, vol. 67, no. 1, pp. 26–35, 1999.

[9] A. Ashkin, "Forces of a single-beam gradient laser trap on a dielectric sphere in the ray optics regime," in *Methods in Cell Biology* (M. P. Sheetz, ed.), vol. 55 (*Laser Tweezers in Cell Biology*), ch. 1, pp. 1–27, Academic Press, 1998.

[10] K. J. Astrom, *Introduction to Stochastic Control Theory*. Academic Press, 1970.

[11] A. T. Bharucha-Reid, *Elements of the Theory of Markov Processes and Their Applications*. McGraw-Hill, 1960.

[12] D. R. Cox and H. D. Miller, *The Theory of Stochastic Processes*. John Wiley, 1965.

[13] A. D. Mehta, M. Rief, J. A. Spudich, D. A. Smith, and R. M. Simmons, "Single-molecule biomechanics with optical methods," *Science*, vol. 283, pp. 1689–1695, 1999.